ISSN 1027-4510, Journal of Surface Investigation: X-ray, Synchrotron and Neutron Techniques, 2019, Vol. 13, No. 3, pp. 434–441. © Pleiades Publishing, Ltd., 2019.
Russian Text © The Author(s), 2019, published in Poverkhnost', 2019, No. 5, pp. 80–88.

Adsorption and Interaction of CO and NO Molecules on Pure and Oxidized Surfaces of Al–Mo(110) Alloy

G. S. Grigorkina[a], A. G. Ramonova[a], V. B. Zaalishvili[b], O. G. Burdzieva[b], and T. T. Magkoev[a, b, *]

[a] *North Ossetian State University, Vladikavkaz, 362025 Russia*

[b] *Geophysical Institute, Vladikavkaz Research Center, Russian Academy of Sciences, Vladikavkaz, 362002 Russia*

**e-mail: t_magkoev@mail.ru*

Received April 15, 2018; revised April 25, 2018; accepted April 25, 2018

Abstract—The coadsorption of carbon-monoxide- and nitric-oxide molecules and their interactions on surfaces of Al–Mo(110) alloy and the system resulting from its oxidation (Al–Mo–O) are investigated using an array of spectroscopic techniques (X-ray photoelectron, Auger electron, infrared, and thermal-desorption spectroscopies), low-energy electron diffraction, and work-function measurements in ultra-high vacuum. Al–Mo(110) alloy is fabricated by the thermal annealing (at 800 K) of an aluminum film several layers thick deposited onto the Mo(110) surface. Aluminum atoms diffuse into the substrate to yield a surface alloy of hexagonal structure characteristic of stoichiometric Al_2Mo alloy. Unlike dissociative adsorption on both Mo(110) and Al(111) surfaces, CO and NO adsorb molecularly at the surface of Al–Mo(110) alloy. At 200 K, the adsorption of CO molecules on the Al–Mo(110) surface containing pre-adsorbed NO molecules has a dramatic effect on the latter by displacing them to higher-coordinated adsorption sites and at the same time causing their molecular axis to tilt toward the adsorbent surface plane. Heating this system to 320 K results in the reduction of nitric oxide by carbon monoxide to yield CO_2 and surface nitrides. This can be a consequence of surface reconstruction that leads to the formation of additional adsorption/reaction sites at the Al/Mo interface and to changes in the substrate's *d*-band filling as a result of alloying. The oxidation of CO by NO proceeds with a markedly higher efficiency at the surface of the Al–Mo–O system; this system results from oxidation of the Al–Mo(110) alloy by oxygen at 700 K and exposure up to 1500 L.

Keywords: surface alloy, aluminum, molybdenum, oxygen, adsorption, surface molecular reactions, carbon monoxide, nitric oxide, surface analysis techniques

DOI: 10.1134/S1027451019030078

INTRODUCTION

In recent years, noble metal-free materials have been intensively studied as alternative cost-effective heterogeneous catalysts [1]. One approach to the development of such materials consists in alloying transition *d* metals from the middle or end of a period with *s* or *sp* elements. In this way, the filling of the *d* band of a transition metal can be increased, whereby the properties of the resulting material approach the characteristics of noble metals, and additional adsorption (and reactive) sites are created at the interface between the alloyed components [2, 3]. For tungsten and molybdenum carbides, this approach enables us to achieve a high—comparable to noble metals—catalytic activity toward CO reduction [4]. Moreover, Mo_2C is used as a stimulator of tungsten carbide-based electrocatalysis in methanol fuel cells [5]. Studies of another alloy (Fe–Co) showed that by varying the ratio of alloying components the intensity of the Fischer–Tropsch process can be controlled, and additionally the rate of the formation of carbides can be suppressed thereby reducing the rate of catalyst degradation [6]. Nonstoichiometric molybdenum nitride has been recognized as another promising catalyst for reactions of the conversion of hydrocarbons and carbon monoxide [7]. Non-stoichiometric molybdenum nitride, in particular, was found to exhibit high catalytic activity upon the selective oxidation of methane to form higher alkanes and alcohols [8]. To reduce the noxious content of vehicle-exhaust gases, much attentions has been paid to catalytic reactions leading to neutralization of the CO + NO mixture [9]. Along with noble metals (Rh, Pt, Pd, and Ir), molybdenum and tungsten carbides were shown to be active catalysts for the neutralization of car exhausts [10, 11]. Despite fairly active research in this direction, systems formed by alloying transition metals from the middle of a period with *sp* elements (e.g., W or Mo with Al) has been virtually unexplored. Actually, we anticipate that such combinations of elements will ensure maximum filling of the *d* band of a transition metal component on account of the high density of free electrons in aluminum and, therefore, enhancement of the catalytic activity of such a material [9]. This hypothesis was

supported by recent studies in which alloying Mo(110) with boron, an element isoelectronic to aluminum, was shown to enhance the catalytic oxidation of CO at the surface of Mo(110) [12]. The aim of this work is to investigate the mechanisms of possible transformations accompanying the adsorption of CO and NO molecules and the interaction between adsorbed molecules at the surface of Al–Mo(110) alloy and Al–Mo–O, a system obtained through in situ oxidation of the latter.

EXPERIMENTAL

Investigations were carried out in a two-level ultra-high vacuum chamber built on the basis of a VGS Escalab MkII system and furnished with an array of surface analysis techniques: X-ray photoelectron spectroscopy (XPS) using a hemispherical analyzer, Auger electron spectroscopy (AES) using a one-stage cylindrical mirror analyzer integrated with a coaxial electron gun, thermal desorption spectroscopy (TDS) using a quadruple mass spectrometer analyzer, infrared (IR) spectroscopy, and low-energy electron diffraction (LEED) using a conventional four-grid concentric hemispherical energy analyzer. The work function ϕ was determined by the Anderson method. For this, a dedicated low-energy electron gun was mounted in the chamber. It was used to record the delay curves in a retarding field formed due to the contact potential difference between the gun's cathode and the sample. In calculating the absolute values for ϕ, the work function for a pure Mo(110) surface was taken to be 5.0 eV. Auger spectra were recorded in the dN/dE mode at an energy of primary electrons of 2 keV and a modulation voltage of 2 V. IR spectroscopy measurements were performed in the grazing-angle configuration using incident plane-polarized radiation at an incidence angle of 85°. This configuration ensures the sensitivity for vibrations in adsorbed molecules with nonzero projection of their dipole moment at the surface normal. In other words, in this variant, IR spectroscopy is sensitive to CO and NO molecules whose axes are aligned with, or tilted with respect to, the surface normal, and it is not sensitive to molecules that lie in the adsorbent surface plane. In recording TDS spectra, a quadruple mass spectrometer with its axis oriented normally to the surface was used as an analyzer, and the temperature of the substrate was increased at a rate of 2 K s^{-1}. The mass spectrometer was configured to simultaneously detect several m/z ratios in desorbing particles.

The surface of a Mo(110) sample was cleaned by conventional annealing at 1700 K in an oxygen atmosphere at a partial pressure of 10^{-7} mbar (this is to remove traces of carbon and sulfur). This was followed by a series of high-temperature pulses in ultra-high vacuum (2×10^{-10} mbar) until all lines due to impurities vanished from the Auger spectra of the sample in all amplification ranges of the spectrometer. An Al film was fabricated on the surface of the Mo(110) sample by thermal sputtering in situ using 99.9999% aluminum in a Knudsen cell. The rate of film growth and the degree θ of surface coverage by the growing film were established by monitoring the weakening of substrate signals in the Auger spectra and from a concentration dependence of the work function $\phi(\theta)$ in the submonolayer range during the sputtering of Al atoms onto the Mo(110) surface. Features of the $\phi(\theta)$ dependence are known to correlate with the coverage of a surface by adatoms [13, 14]. Considering the sizes of Mo and Al atoms, the concentration of aluminum atoms in a single layer, i.e., at $\theta = 1$, was taken to be 1.5×10^{15} cm^{-2} [14]. As is known, an aluminum film up to a few single layers thick has the Al(111) structure on the Mo(110) surface, but disorder occurs in thicker films [14, 15]. To obtain an Al–Mo(110) surface alloy, a two-single-layer thick aluminum film deposited onto the Mo(110) surface was annealed at 800 K for 3 min. The formed alloy was stable during annealing up to a temperature of 1300 K. For adsorption experiments, CO and NO were supplied to the ultra-high vacuum chamber to a partial pressure of around 10^{-7}–10^{-8} mbar. The surface exposure to gas molecules was 1 L (langmuir; 1 L = 10^{-6} Torr s^{-1}) at a partial pressure of the corresponding gas of 10^{-6} Torr for 1 s. To differentiate between TDS signals due to CO and N_2 (both have an m/z ratio of 28), we used isotope-labeled nitric oxide ^{15}NO. The sample holder allowed cooling with liquid nitrogen to a temperature of 90 K. To create the Al–Mo–O oxide system, the Al–Mo(110) alloy fabricated as described above was exposed to dioxygen which was supplied to the ultra-high vacuum chamber to a partial pressure of 5×10^{-10} mbar until an exposure of 1500 L was reached at a substrate temperature of 700 K. The adsorption of CO and NO molecules on the surface of the Al–Mo–O system was initiated after the supply of oxygen had been stopped and the substrate had been cooled to 90 K.

RESULTS AND DISCUSSION

The variation in the work function $\phi(\theta)$ with coating of the Mo(110) surface, maintained at room temperature, by aluminum atoms is shown in Fig. 1. The initial decrease in the work function is suggestive of the electropositive character of adsorption due to polarization of the chemisorbed charge Al–Mo into the substrate. This is supported by the shape of the $\phi(\theta)$ dependence: after the work function reaches a minimum, it plateaus when a single-layer coating is reached. This shape is typical of alkaline and alkaline-earth metals, which nearly always exhibit electropositive adsorption behavior [16]. We note that, despite intensive research into the adsorption of metal atoms on metal substrates, the adsorption of Al onto the Mo(110) surface, as well as other refractory metals, remains little studied. A concentration dependence

similar to the one in Fig. 1 was reported earlier in one of a few studies on the subject (Kolashkevich *et al.*, [14]). A value of 0.19 D for a dipole moment μ of Al adatoms, which is in line with the value reported in [14] (0.182 D), was obtained from the $\phi(\theta)$ dependence by extrapolation to zero ($\theta \to 0$) and using the Helmholtz relationship $\Delta\phi = 4\pi\theta e\mu$. At room temperature, the aluminum film growing layer-by-layer on the Mo(110) surface has the Al(111) structure [13, 14]. Annealing causes aluminum atoms to diffuse into the substrate to form an alloy [14], which is accompanied by an increase in the work function from 4.15 to 4.4 eV. As was shown earlier [17], annealing a thin-film Al–Mo system caused the mutual diffusion of its constituents and yielded $MoAl_{12}$ alloy. Generally, alloying Al and Mo gives 12 equilibrium phases [18]. Ivkov et al. [19], however, showed that thin-film alloys Al_xMo_{100-x}, with x varying in a broad range, can be obtained. Auger spectra and LEED patterns were recorded for a bilayer Al film created on the surface Mo(110) before and after annealing (the structure) at 800 K are shown in the inset in Fig. 1. The LEED data show that before annealing aluminum had the Al(111) structure. The observed decrease in the intensity of the aluminum signal on Auger spectra is suggestive of its diffusion into the substrate. Also, the shift in the energy of the *LVV* Auger transition for Al by 1.5 eV toward lower kinetic energies indicates that a chemical interaction occurred between the Al and Mo atoms. According to the obtained diffraction pattern acquired after annealing, the surface underwent reconstruction to form the $(\sqrt{3} \times \sqrt{3})R30°$ structure. For annealing an Al film on a Ru(1000) surface, Campbell and Goodman [20] obtained a similar LEED pattern, which they interpreted as due to the slightly distorted hexagonal densely packed surface of Al_2Ru. This alloy is characterized by an orthorhombic structure with alternating planes with hexagonal symmetry consisting of an ordered mixture of Al and Ru atoms, which correspond to an Al coating of 2/3. Upon the formation of such a surface alloy due to annealing, the excess of aluminum diffuses in the substrate bulk. Considering the similarity between the diffraction patterns obtained here and in Campbell and Goodman's work [20], as well as similar lattice constants for the Mo and Ru basal planes, we can assume that a surface alloy of a similar type is formed in the case of the Al–Mo(110)–Al_2Mo system. This assumption is corroborated by an increase in the work function from 4.15 to 4.4 eV, which, according to the dependence $\phi(\theta)$ (Fig. 1), corresponds to a coating of 0.55, a value close to the aluminum content in the Al_2Mo alloy, 0.67 [20].

Alloying usually leads to substantial changes in the electron structure of alloying components, in particular, the filling of the transition metal's *d* band increases and its center effectively shifts down relative to the Fermi level on account of charge transfer from the more electropositive metal [2, 9]. Apart from changing the atomic structure of the substrate, this may have a big impact on the adsorption process and the transformation of molecules at the surface. As we mentioned above, CO and NO are two benchmark molecules that are used most commonly in studies of the adsorption and catalytic properties of various substrates. The IR spectra of CO and NO molecules adsorbed separately (exposure, 20 L) onto the surface of Al–Mo(110) alloy maintained at 200 K are shown in Fig. 2. Both spectra feature a single band at 2026 cm^{-1} for CO and 1753 cm^{-1} for NO, which correspond to the intramolecular vibrations C–O and N–O, respectively. However, no absorption bands were seen in the IR spectra in case of adsorption onto Mo(110) and Al(111) surfaces. This can be attributed to the dissociation of these molecules on both the Mo(110) and Al(111) surfaces [21]. We thus see that by alloying Mo(110) with Al, the adsorption properties of the substrate changed cardinally. Similarly, Ren *et al.* [22] found that the dissociation of NO molecules was fully suppressed upon the formation of a compound between molybdenum and carbon. The same picture was observed for alloying Pd(111) with Al [23]. According to the accepted viewpoint, these effects are explained by an increase in the filling of the transition metal's *d* band and effective lowering of its center, as well as a decrease in the density of states at the Fermi level. According to the known Blyholder model [24], this reduces charge transfer from the substrate's *d* zone onto the $2\pi^*$ anti-bonding orbitals in CO and NO molecules. The wavenumbers obtained for the absorption peaks (Fig. 2, spectra *1* and *2*) suggest that both types of molecules are oriented perpendicularly to the surface, with their oxygen atoms pointing away from the surface [25]. Adsorption sites with higher coordination, e.g., bridged, tetrahedral, or octahedral sites, are characterized by considerably lower wavenumbers [25]. Apparently, the fact that no molecules were bonded to the surface in this way can be attributed to the blocking of corresponding adsorption centers at the Mo(110) surface by aluminum atoms as a result of alloying. Studies by Campbell and Goodman [20] indicate that it is these high-coordination lattice nodes that are occupied by aluminum atoms during alloy formation. At the same time, we should not discount the possibility that the adsorption properties of the substrate were affected by changes in its electronic structure as a whole. A similar effect was observed, in particular, in alloying Pt(111) with small amounts of Ge (5%) [26]: the properties of the thus-modified Pt(111) surface toward the adsorption of CO and NO changed markedly due to changes in the electronic structure of the resulting alloy.

The IR absorption spectrum recorded during the adsorption of CO (20 L) onto the Al–Mo(110) surface containing pre-adsorbed NO (20 L) is shown in Fig. 3 (spectrum *3*). The corresponding Auger spectrum shown in Fig. 3 (spectrum *1*) features signals due to Al, Mo, C, N, and O. We can see that the coadsorption of

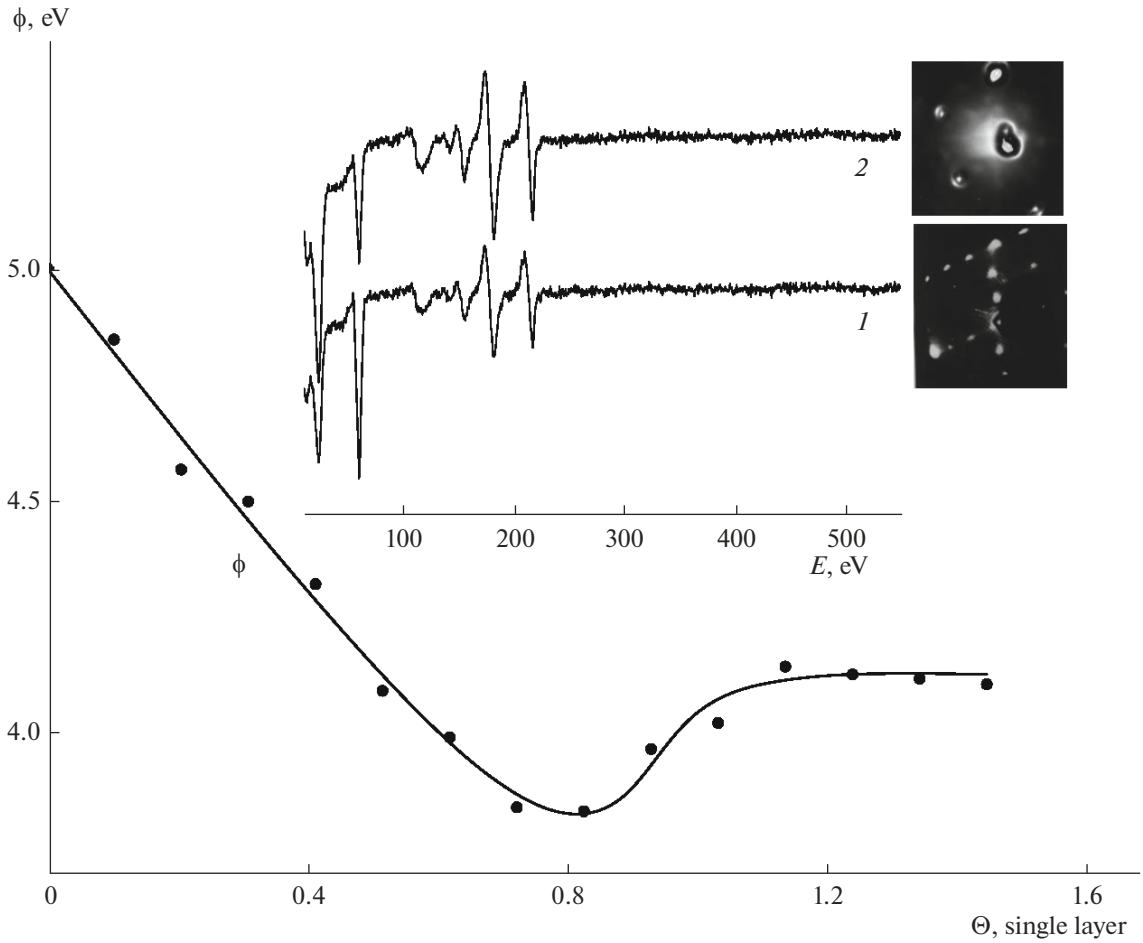

Fig. 1. Dependence of the work function on the surface coverage of the Mo(110) surface at room temperature by aluminum atoms. The inset shows the Auger spectra and LEED patterns of two-layer-thick aluminum films (spectrum *1*) before and (spectrum *2*) after annealing at 800 K for 3 min.

CO and NO molecules has specific features that were not seen in the case of the individual adsorption of these gases: a considerable shift in the vibrational features toward lower wavenumbers occurred (250 and 40 cm^{-1} for NO and CO, respectively). The wavenumber observed for NO (1506 cm^{-1}) is characteristic of molecules adsorbed in bridged and hollow adsorption sites, while the value obtained for CO corresponds to linearly adsorbed molecules [25]. In the case of coadsorption, the lower intensity of vibrational signals due to NO and CO, as compared to the case of individual adsorption of these gases, can be ascribed to the tilted geometry of the adsorbed layer. This explains the indicated red shift in the wavenumber for the CO molecule: while remaining adsorbed in the linear geometry, the molecule deviates from the surface normal. The situation with the NO molecule changes more radically: in addition to deviation of the molecular axis from the surface normal, the molecule changes its linear adsorption site to a bridge or a hollow one. With only one vibrational feature of NO adsorbed at the Al–Mo(110) surface (Fig. 2, spectrum *2*) which corresponds to the occupation of only linear adsorption sites, we conclude that adsorption sites with higher coordination or hollow adsorption sites are not preferred adsorption sites. Subsequently coadsorbed CO molecules, however, have a marked impact on the (adsorbed) NO molecules: the latter are displaced from linear to bridge or hollow sites and at the same time their molecular axes tilt toward the adsorbent surface plane. By moving to such higher-coordinated sites, the NO molecule is prone to a stronger interaction with both Mo and Al, which causes a reverse charge transfer from the adsorbent surface to the $2\pi^*$ anti-bonding orbital in NO thereby weakening its intramolecular bond. The fact that the NO molecule changes the type of its adsorption site as a result of subsequent CO adsorption was also reported in [27] for the system Ni/MgO(111). A similar effect was also seen for the (NO + CO) system on the Ni(111) surface [28]. Slight heating of the (NO + CO)/Al–Mo(110) system to a temperature of 350 K resulted in the disappearance of all vibrational features in the IR spectra. In the Auger spectrum recorded for this situation

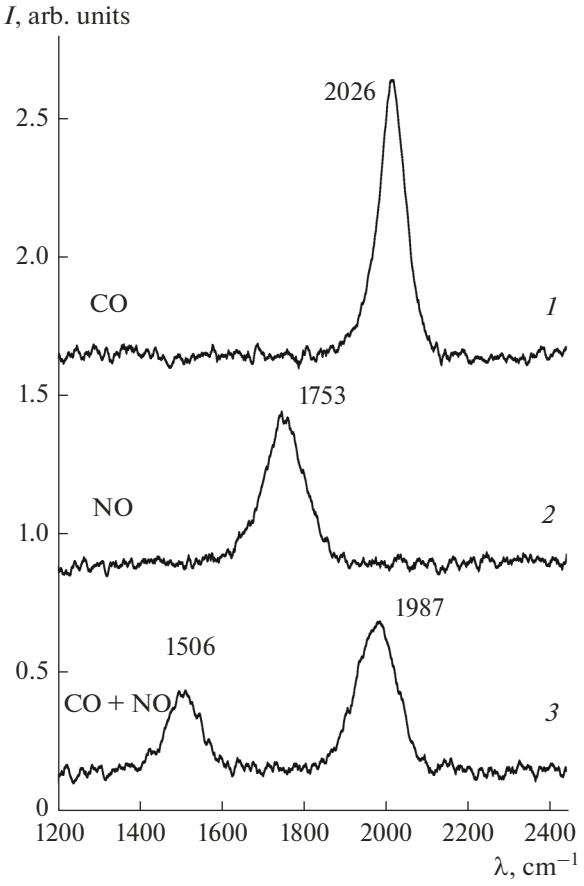

Fig. 2. IR spectra of CO and NO molecules adsorbed either (spectra *1* and *2*) separately or (spectrum *3*) joint at the Al–Mo(110) alloy surface maintained at 200 K. IR spectrum *3* is for the adsorption of CO molecules on the surfaces with pre-adsorbed NO molecules.

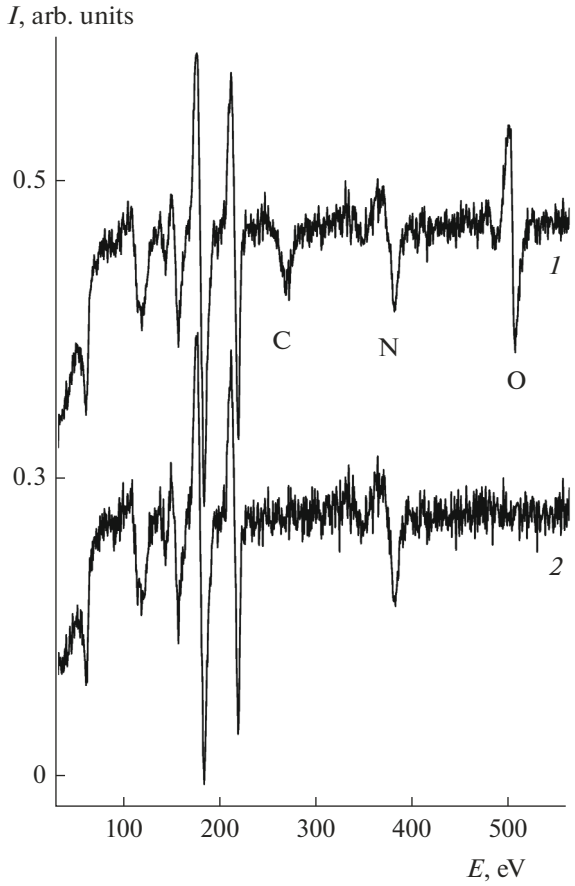

Fig. 3. Auger spectra of the (CO + NO)/Al–Mo(110) system (spectrum *1*) maintained at a temperature of 200 K and (spectrum *2*) after annealing at 380 K. To highlight the energy shift in the Auger peak due to annealing, the N region of the *KLL* Auger signal is shown.

(Fig. 3, curve *2*), the signals due to C and O nearly vanished, while the signal due to N remained virtually unchanged, except its shift by 1.6 eV toward higher kinetic energies.

The TDS spectra for the systems characterized by IR spectrum *3* in Fig. 2 and the Auger spectrum *1* in Fig. 3 are shown in Fig. 4. As can be seen, these spectra feature signals due to only CO ($m/z = 28$) and CO_2 ($m/z = 44$). These observations suggest that a portion of the CO molecules transformed into CO_2 during heating, presumably on account of NO reduction. This process is well-known, e.g., heating of the (NO + CO)/Rh system gives rise to CO_2 and N_2 [29]. The dissociation of NO can be postulated to be the first stage in this process. This supposition is based on the results of previous studies of (CO + NO) systems at the surfaces of molybdenum and tungsten carbides, which showed the almost complete dissociation of NO molecules, but not CO ones [10, 11]. In our case, IR spectroscopy indicates that the NO molecule is in a predissociative state (Fig. 2, spectrum *3*). While in a highly coordinated adsorbed state, the NO molecule is acted upon by both Mo and Al, the two materials that adsorb NO dissociatively. The coadsorbed CO molecules that also have a tilted orientation, which can be regarded as their pre-reaction state, interact with oxygen released during NO dissociation. Instead of the anticipated recombination to form N_2, nitrogen atoms are bonded to the substrate, as indicated by a shift in the position of the *KLL* line of N in the Auger spectrum shown in the inset in Fig. 3. According to previous studies that revealed the high catalytic activity of aluminum and molybdenum nitrides for the conversion of CO [7, 8, 30, 31] the resulting substrate, i.e., Al/Mo(110)/N, can exhibit activity in CO oxidation. The fact that oxygen resulting from NO dissociation oxidizes CO, and not Al or Mo, can be a consequence of O and N atoms competing for adsorption sites: for instance, it is known that nitrogen can replace oxygen in aluminum oxide to give AlN [32]. The marked transformation of the adsorption and reactive properties of CO and NO molecules caused by alloying Al with Mo(110) can be ascribed, on the one hand, to surface reconstruction and, on the other, to alterations

in the electronic structure of the alloy as a whole. Surface reconstruction to form the $(\sqrt{3} \times \sqrt{3})R30°$ structure results in the emergence of low-coordination adsorption sites and interfacial adsorption sites at the Al/Mo interface. The presence of the aforementioned low-energy vibrational band at 1506 cm^{-1} indicates that these are sites of the preferential adsorption of NO molecules. Additionally, alloying leads to lowering of the effective center of the substrate's *d* band relative to the Fermi level, which has a big impact on the redistribution of intramolecular charge in NO and CO molecules upon adsorption [33].

Figures 5b and 5c show the XPS spectra (marked *1*) for the system resulting from exposure of the Al–Mo(110) alloy heated to 700 K to oxygen (partial pressure, 5×10^{-7} mbar). A more informative interpretation of the spectra of the Al–Mo–O system was achieved by comparing them to the spectra of aluminum and molybdenum oxides. To this end, we made use of well-known techniques for (i) the *in situ* oxidation of aluminum films sputtered onto the Mo(110) surface, which leads to the formation of Al_2O_3 and (ii) direct oxidation of the Mo(110) surface to form MoO_2 [34, 35]. The spectra of the thus-prepared Al_2O_3 and MoO_2 are shown in Figs. 5a and 5b (spectra *2*). The spectra of metallic aluminum and molybdenum are also provided for comparison (spectra *3*). By comparing spectra *1* and *2* (Fig. 5a), we recognize that the electronic state of aluminum atoms in the oxidized form of the alloy, Al–Mo–O, is nearly identical to that in aluminum oxide Al_2O_3. At the same time, we see (Fig. 5b) that the state of Mo atoms in the Al–Mo–O system (spectrum *1*) is markedly different from that in MoO_2 (spectrum *2*). The observed correspondence of the spectral profiles and the Mo 2*p* lines between the Al–Mo–O system (spectrum *1*) and Mo (spectrum *3*) indicates that, in contrast to Al atoms, the state of Mo atoms in the ternary system resembles that in metallic Mo. At the same time, slight differences between spectra *1* and *3* (Fig. 5b), such as a slight shift in the line positions toward higher bond energies and line broadening, tell us that oxidation of the Al–Mo(110) alloy causes some transformation of the electronic state of Mo atoms, albeit to a considerably lesser extent than in case of Al. These results suggest that the interaction between the Al–Mo(110) alloy and oxygen leads, on the one hand, to nearly complete oxidation of aluminum to Al_2O_3, and to insignificant changes in the state of Mo atoms, on the other. In view of the formation of ternary compounds, we can hypothesize the formation of nonstoichiometric molybdenum aluminate $Mo_{1-x} \times nAl_2O_3$ at the surface, in which the states of molybdenum and aluminum are qualitatively similar to those in the Al–Mo–O system [36]. The LEED data suggest that the surface of this system does not have long-range order, i.e., oxidation leads to amorphization of the initially ordered structure of the Al–Mo(110) system.

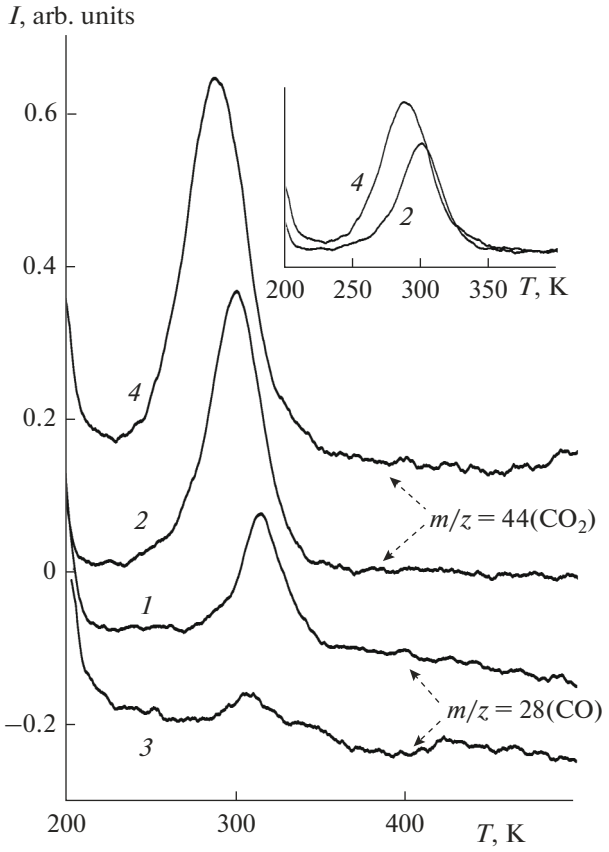

Fig. 4. TDS spectra of CO and CO_2 systems formed as a result of adsorption after exposure of (spectra *1* and *2*) the Al–Mo(110) and (spectra *3* and *4*) Al–Mo–O surfaces containing pre-adsorbed NO molecules to 20 L of CO (exposure for pre-adsorption, 20 L). By way of illustration, the inset shows the intensity ratio for CO_2 lines for (spectrum *2*) Al–Mo(110) and (spectrum *4*) Al–Mo–O.

Oxidation of the surface of Al–Mo(110) alloy leads to noticeable changes in the way adsorbed CO and NO molecules interact. This can be demonstrated by comparing the TDS spectra of (CO + NO) on the Al–Mo(110) surface (Fig. 4, spectra *1* and *2*) to those of (CO + NO) on the Al–Mo–O surface (Fig. 4, spectra *3* and *4*). We can see that the conversion of CO to CO_2 occurs with a markedly higher efficiency on the surface of the oxidized system (i.e., Al–Mo–O) than on the surface of Al–Mo(110) alloy: the intensity of the signal due to CO_2 is higher in spectrum *4* than in spectrum *2*, and the signal due to the desorption of CO recorded in spectrum *3* is barely seen in spectrum *1*. The Al–Mo–O system under study can be regarded as a model system representing the metal-oxide system Mo/Al_2O_3, which exhibits superior catalytic performance due to the special characteristics of metal species in contact with the oxide and the properties of the metal/oxide interface [37]. That being so, the Al–Mo(110) and Al–Mo–O systems can be consid-

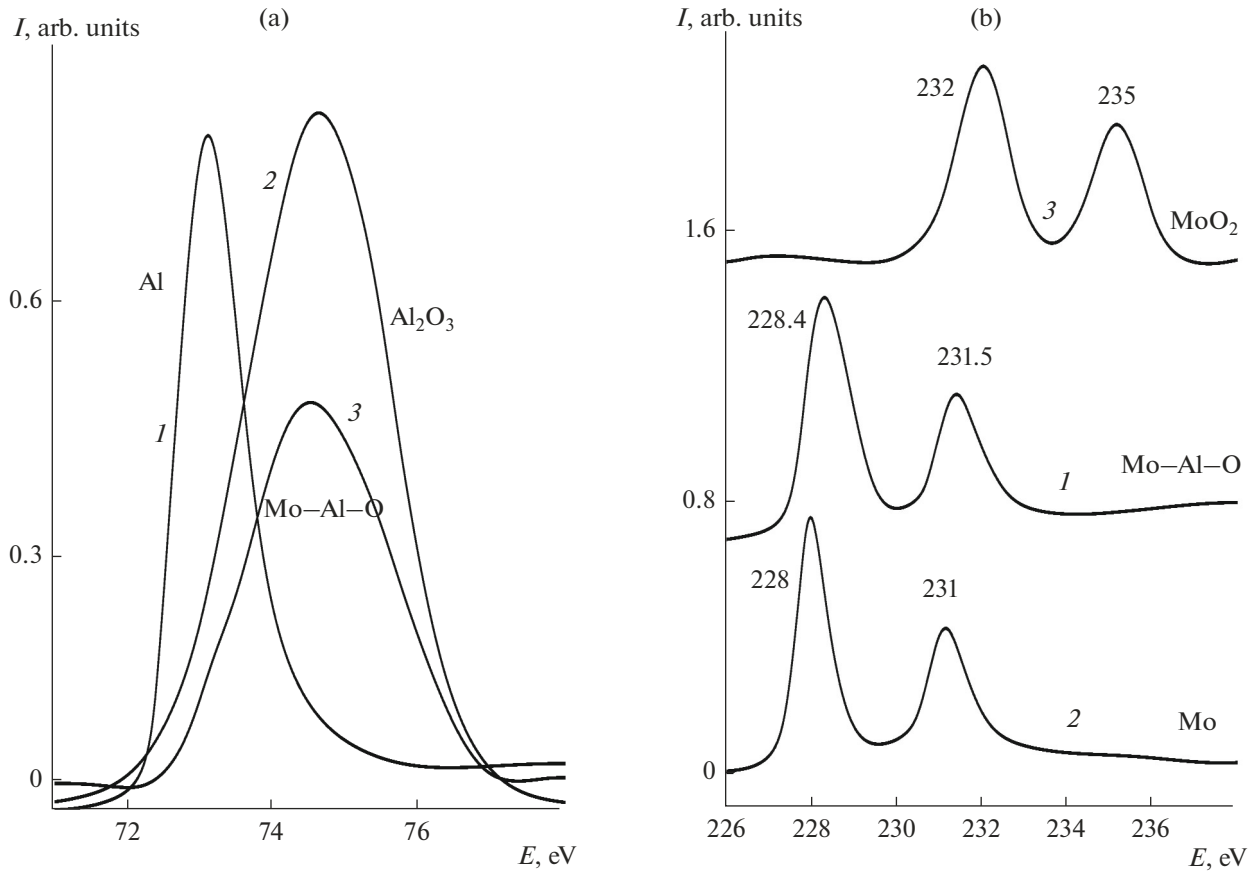

Fig. 5. (a) Al 2*p* peaks in the XPS spectra for (spectrum *1*) the Al–Mo–O system; (spectrum *2*) an Al_2O_3 film, around 10 nm thick, on the Mo(110) surface, obtained by reactive sputtering; and (spectrum *3*) an 8 nm-thick aluminum film on the Mo(110) surface. (b) Mo 3*d* peaks in XPS spectra for (spectra *1*) the Al–Mo–O system, (spectrum *2*) molybdenum oxide MoO_2 obtained by oxidation of Mo(110) by oxygen, and (spectrum *1*) Mo(110).

ered as an alternative to platinum-based catalysts for the neutralization of a (CO + NO) mixture.

CONCLUSIONS

Annealing a two-single-layer aluminium film on the Mo(110) surface at 800 K leads to the formation of the $MoAl_2$ surface alloy of hexagonal symmetry with a relative surface concentration of Al of 2/3. In contrast to the dissociative adsorption at aluminium or molybdenum, NO and CO molecules adsorb molecularly on the surface of this alloy cooled to 200 K. The adsorption of CO molecules on the Al–Mo(110) surface containing pre-adsorbed CO molecules has a marked effect on the latter by moving them to higher-coordinated bridge and/or hollow sites and at the same time causing their molecular axis to tilt toward the adsorbent surface plane. Heating this system to 320 K leads to reduction of the adsorbed nitric oxide, the formation of surface nitrides, the oxidation of CO, and the desorption of resulting CO_2 molecules into the gaseous phase. The substantial transformation of the adsorption properties and reactivity of CO and NO, as a result of alloying Al with Mo(110), can be ascribed to both surface reconstruction and changes to the electronic structure of the alloy as a whole. The oxidation of CO by NO proceeds with a markedly higher efficiency at the Al–Mo–O surface.

ACKNOWLEDGMENTS

The work was supported within state assignment (project no. 3.9281.2017) by the Ministry of Education and Science of the Russian Federation and by the Russian Basic Research Foundation (project no. 19-47-02010).

REFERENCES

1. P. Du and R. Eisenberg, Energy Environ. Sci. **5,** 6012 (2012).
2. J. A. Rodriguez, Surf. Sci. Rep. **24,** 223 (1996).
3. J. L. Whitten and H. Yang, Surf. Sci. Rep. **24,** 55 (1996).
4. K.-Z. Qi, G.-C. Wang, and W.-J. Zheng, Surf. Sci. **614,** 53 (2013).

5. H. H. Hwu and J. G. Chen, Surf. Sci. **536,** 75 (2003).
6. P. Rochana and J. Wilcox, Surf. Sci. **605,** 681 (2011).
7. J.-G. Choi, R. L. Cur, and L. T. Thompson, J. Catal. **146,** 218 (1994).
8. M. K. Awad and A. B. Anderson, Surf. Sci. **218,** 543 (1989).
9. V. P. Zhdanov and B. Kasemo, Surf. Sci. Rep. **29,** 31 (1997).
10. J. Wang, M. Castonguay, J. Deng, and P. H. McBreen, Surf. Sci. **374,** 197 (1997).
11. J. Brillo, R Sur., H. Kuhlenbeck, H.-J Freund, Surf. Sci. **397,** 137 (1998).
12. I. V. Tvauri, S. A. Khubezhov, Z. S. Demeev, et al., Vacuum **88,** 8 (2013).
13. R. J. Baierle, T. M. Schmidt, and A. Fazzio, Solid State Commun. **42,** 49 (2007).
14. J. Kolaczkiewicz, M. Hoch, and S. Zuber, Surf. Sci. **247,** 284 (1991).
15. A. G. Jackson and M. P. Hooker, Surf. Sci. **28,** 373 (1971).
16. J. P. Muscat and D. M. Newns, Solid State Commun. **11,** 737 (1972).
17. R. N. Singh, D. M. Brown, M. J. Kim, and G. A. Smith, J. Appl. Phys. **58,** 4598 (1985).
18. L. Brewer and R. H. Lamoreaux, in *Binary Alloy Phase Diagrams,* **vol. 1**, Ed. by T. B. Massalski, J. L. Murray, L. H. Bennett, and H. Baker (American Society of Metals, Ohio, 1987), p. 133.
19. J. Ivkov, K. Salamon, N. Radic, and M. Soric, J. Alloys Compd. **646,** 1109 (2015).
20. C. T. Campbell and D. W. Goodman, J. Phys. Chem. **92,** 1021 (1988).
21. C. R. Henry, Surf. Sci. Rep. **31**, 231 (1988).
22. J. Ren, J. Wang, C. -F. Huo, et al., Surf. Sci. **601,** 1599 (2007).
23. V. Matolin, I. Stara, N. Tsud, and V. Johanek, Prog. Surf. Sci. **67,** 167 (2001).
24. B. Hammer, Y. Morikawa, and J. K. Norskov, Phys. Rev. Lett. **76,** 2141 (1996).
25. F. M. Hoffmann, Surf. Sci. Rep. **3,** 107 (1983).
26. K. Fukutani, T. T. Magkoev, Y. Murata, and K. Terakura, Surf. Sci. **363,** 185 (1996).
27. T. T. Magkoev, Solid State Commun. **132,** 93 (2004).
28. A. Beniya, N. Isomura, H. Hirata, and Y. Watanabe, Surf. Sci. **613,** 28 (2013).
29. R. E. Hendershot and R. S. Hansen, J. Catal. **98,** 150 (1986).
30. R. Toyoshima, M. Yoshida, Y. Monya, et al., Surf. Sci. **615,** 33 (2013).
31. R. Wichtendahl, M. Rodriguez-Rodrigo, U. Hartel, et al., Surf. Sci. **423,** 90 (1999).
32. M. Saito and R. B. Anderson, J. Catal. **63,** 438 (1980).
33. J. A. Schaidle and L. T. Thompson, J. Catal. **329,** 325 (2015).
34. P. J. Chen and D. W. Goodmann, Surf. Sci. **312,** L767 (1994).
35. K. Radican, N. Berdunov, and I. V. Shvets, Phys. Rev. B **77,** 085417 (2008).
36. P. M. Natishan, E. McCafferty, and G. K. Hubler, Corros. Sci. **32,** 721 (1991).
37. Y. Wang, F. Gao, and W. T. Tysoe, Surf. Sci. **590,** 181 (2005).

Translated by A. Kukharuk